Ninth International Conference on Computational Fluid Dynamics (ICCFD9), Istanbul, Turkey, July 11-15, 2016 **ICCFD9-2016-185**

Investigation of the Mechanical Integrity of Wings/Fins under Thermal Loading

Emir ÖZKÖKDEMİR[1], Dilek Funda KURTULUŞ[2]

[1] Roketsan Missile Inc., Ankara, Turkey
[2] Department of Aerospace Engineering, METU, Ankara, Turkey

Corresponding author: emirozkokdemir@gmail.com

Abstract: Wings or fins are exposed to a variety of loading during fight at supersonic and hypersonic regime. Thermal loading is one of the most important loading type is highly effective on the structure of wings/fins. Temperature gradient formed by thermal loading may cause deformation on the wings/fins. Structural integrity of wings/fins under thermal loading as aerodynamic heating were investigated in this work. NACA 0012 airfoil profile was selected as two dimensional analysis models. A set of analysis includes computational fluid dynamic (CFD) analysis part and finite element (FE) analysis part had done and results were compared with the test data from literature. The current study aims to obtain deformation rates of fins exposed to the high temperatures. The heat transfer coefficient and static temperature on the airfoil in addition to the pressure distribution result a deformation on the airfoil. This deformation is calculated by use as a commercial finite element code.

Keywords: Aerodynamic Heating, Computational Fluid Dynamics, Finite Element Methods.

1 Introduction

Aerodynamic heating is one of the most important design considerations on the wings/fins and can be obtained basically in three ways; with heat flux measurement during flight test, with computational fluid dynamic analysis and with empirical correlations. Temperature gradient formed by thermal loading may cause deformation on the wings/fins. Structural integrity of wings/fins under thermal loading as aerodynamic heating was investigated in this work. Some of studies about wings/fins in the literature are represented below.

Sheldahl et al. [1] from Sandia National Laboratories investigated the 6-in (152mm) and 15-in (381mm) chord NACA 0012 model that was tested at between Reynolds numbers of 10^4 to 10^7 through angles of attack of 0º to 180º degrees. Aerodynamic coefficients from the CFD analysis are compared with the test data

Wright et al. [2] dealt with wing concepts, a delta and an arrow wing, were compared by examination of cruise efficiency, structural weight, and aerodynamic characteristics supported by available wind-tunnel data. Mission range was the figure of merit in the comparison. The study had shown that the arrow wing has the greatest range potential for commercial supersonic cruise vehicle. The effects of aircraft operating constraints make the arrow wing the preferred planform compared to the delta wing planform.

In the study of Sani et al. [3], rarefied supersonic and subsonic gas flow(at different angles of attacks and Knudsen numbers) around a NACA 0012 airfoil is simulated using both continuum and particle approaches. They investigated variations of the lift and the drag coefficients with angles of attacks and Knudsen numbers. Their results showed that drag coefficient increases with the Knudsen number and lift coefficient agreed with the linearized theory. In addition to this, it was obtained that the deviation starts as soon as the angle of attack goes beyond 15° or shock wave forms above the airfoil.

Martinat et al. [4] studied about the NACA 0012 dynamic stall at Reynolds numbers 10^5 and 10^6 for two and three dimensional simulations. The aim of their study is to evaluate the turbulence modelling performance by comparing classical and advanced URANS approaches in two- and three-dimensional simulations. As a result in the study, the k-ε Chien model provided the best results comparing Spalart and Allmaras model for the case of a Reynolds 10^5 pitching airfoil and advanced turbulence models (like Organised Eddy Simulation and SST k-ω) have shown better results than classical models (URANS) for dynamic stall prediction. Also it was obtained that two-dimensional simulations are useful for fast pre-design use, because they are able to capture a significant part of the structure dynamics compared to the three-dimensional simulations.

Yemenici [5] investigated the flow field around NACA0 012 airfoil experimentally. Test was done in a wind tunnel under the effects of Reynolds number and angle of attack. The results showed that the pressure coefficient of the suction side of the airfoil initially increased near the leading edge and then showed a monotonously decrease up to trailing edge for all angle of attack and the angles of stall and lift coefficients increased with Reynolds number.

Prediction of laminar/turbulent transition was investigated in the study of Johansen [6] from Risø National Laboratory. The more general e^n transition prediction technique was compared to an early developed technique from Michel [7]. NACA 0012 airfoil with SST k- ω turbulence model was used to validate the transition models. The computations of the NACA 0012 airfoil at high Reynolds number show a minor effect on the lift prediction while the drag characteristics are more influenced.

In the study of Miller et al. [8], design of a supersonic cruise fighter wing was investigated. Firstly, wing geometry was simplified to research wind tunnel test geometry, then optimum wing design was obtained according to wind tunnel test results. Tests were repeated by three wing configurations; flat wing, the fully cambered wing and flat wing with leading edge flaps. For Mach number 2.0 and the range of lower lift coefficients, the test model drag is reduced by over 30 percent and the cambered wing produces a three count drag improvement over the flat wing.

Nangia et al. [9] studied about the class of thin supersonic wings with low sweep. The aim of their study was to improve the low speed (about Mach number 2.0) performance using leading edge flaps. Two planforms were investigated. One was for Mach 2.4, another one was for Mach 2.0. They obtained that a sharp leading edge wing without leading edge deflection gives Cd close to Cl tanα. (α is the angle of attack)

Sakata et al. [10] dealt with the design study of an arrow wing of supersonic-cruise aircraft. An analytical study was performed to determine the best structural approach for design of wing of a Mach number 2.7. The design consideration of their study was basically aerodynamic loads and material selection. According to the results, a hybrid wing structure was the most efficient material for their design purpose.

Winter et al. [11] studied a multidisciplinary design process of a conventional and oblique wing configurations at Mach 1.6. The aim of their study compared the aerodynamic performance of an oblique wing body configuration with a traditional symmetrical swept wing. It is obtained that oblique configurations achieve cruise performance similar to performance of conventional designs while providing low speed performance and the oblique wing designs showed little advantage in cruise performance, but the low speed performance is exceptional and leads to an interesting design concept.

In the study of Hoffman et al. [12] three dimensional unsteady high Reynolds number flow simulations of NACA 0012 wing profile were investigated for a range of angles of attack. Computational predictions of aerodynamic forces were validated against experimental data. A stabilized finite element method was used. It is found that the finite element simulations correctly capture the basic flow features found in experiments. Their simulations captured the stall with dramatically reduced lift over drag ratio.

2 Problem Statement

2.1 Governing Equations and Geometry

The governing equations are Navier-Stokes equations for compressible, two dimensional flow:

$$\frac{\partial(\rho u)}{\partial t} + \mathrm{div}(\rho u \mathbf{u}) = -\frac{\partial p}{\partial x} + \mathrm{div}(\mu \,\mathrm{grad}\, u) + S_{M_x}$$
$$\frac{\partial(\rho v)}{\partial t} + \mathrm{div}(\rho v \mathbf{u}) = -\frac{\partial p}{\partial y} + \mathrm{div}(\mu \,\mathrm{grad}\, v) + S_{M_y}$$
$$\frac{\partial(\rho w)}{\partial t} + \mathrm{div}(\rho w \mathbf{u}) = -\frac{\partial p}{\partial z} + \mathrm{div}(\mu \,\mathrm{grad}\, w) + S_{M_z}$$

where S_M is momentum source, Φ is dissipation function, $\mathbf{u}$ is the velocity vector, ρ is the fluid density, p is the pressure, μ is the dynamic viscosity. ANSYS Fluent implements the finite-volume method to solve conservation equations [13]. The pressure-velocity coupling is done by means of the SIMPLE-type fully implicit algorithm.
The flow around NACA 0012 airfoil was obtained at Re=6 x 10^6 turbulent external conditions. The thickness distribution of NACA 4 digit airfoils, y_t, was found by using [14, 15].

$$y_t = \pm\frac{t/c}{0.2}(0.2969x^{0.5} - 0.126x - 0.3516x^2 + 0.2843x^3 - 0.1015x^4)$$

where x∈[0 1] and t/c is the maximum thickness to chord ratio, which is in percentage last two digits of NACA 4 digit airfoils. In the CFD part of study, 6in (152mm) chord NACA 0012 airfoil profile was used as wing profile. Cosine spacing was used in the generation of points at the leading and trailing edge. NACA 0012 airfoil is a symmetric airfoil so the thickness distribution is sufficient for the upper and lower surface definitions.

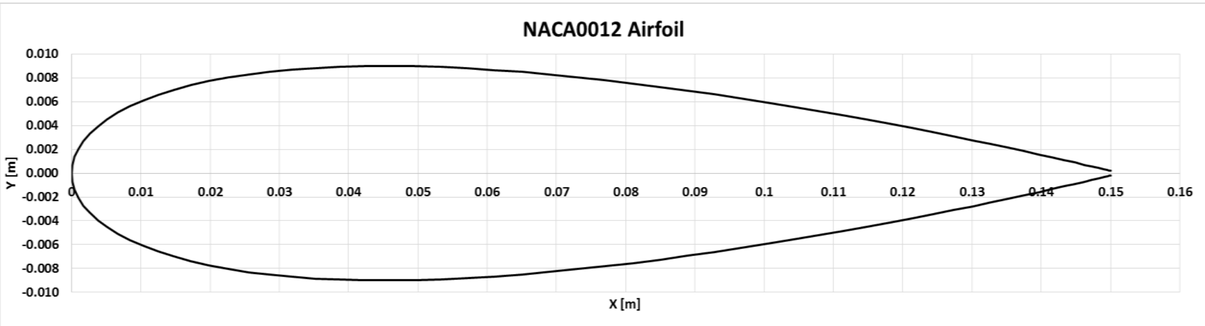

Figure 1: NACA 0012 Airfoil Surface

The pressure far field inlet boundary condition was used at two inlet sections of the outer domain and pressure outlet was used at the outer region. The pressure outlet boundary was located at 50c away from trailing edge of the airfoil and the far field boundary conditions were located 20c away from other sides of the airfoil. The domain generated for CFD part of the study is given in Figure 2.

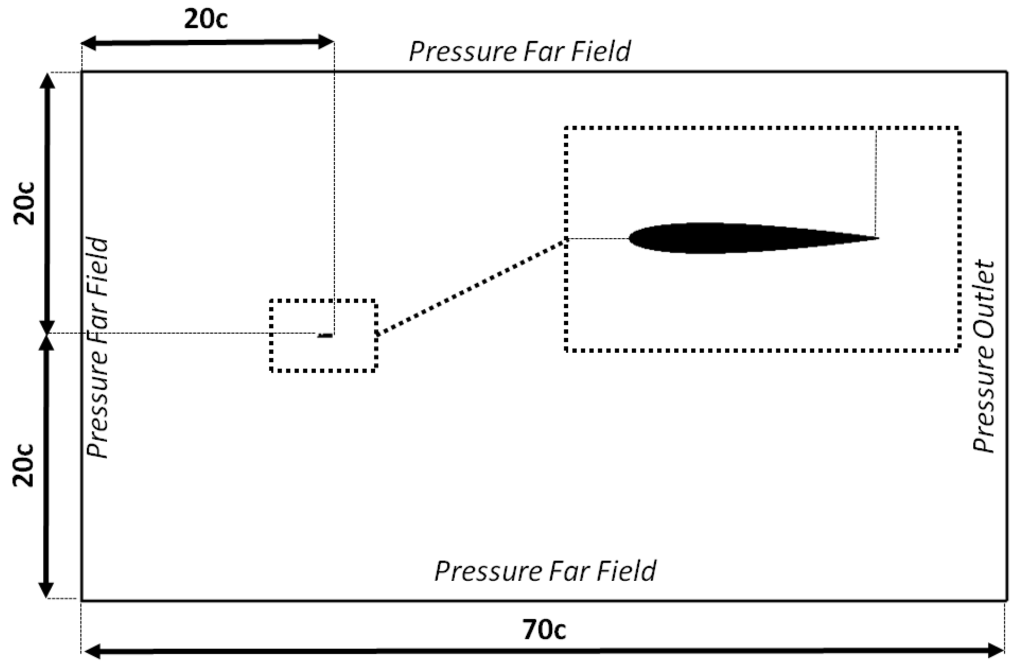

Figure 2: Domain for CFD Analysis Part

2.2 Grid Refinement Study

Detailed grid refinement studies were carried out for three different meshes were used. Geometry and mesh were generated by using commercial grid generation software so that the boundary shapes and number of nodes and elements could be adjusted for all cases with an almost equal accuracy. The level 1 mesh consisted of 120 nodes, level 2 mesh 240 nodes and level 3 mesh 480 nodes around the airfoil. Total numbers of elements in the domain are given in Table 1. The first cell spacing of the boundary layer had value of 4.22 x 10^{-6}c for all mesh levels. The mesh regions for all mesh levels are demonstrated in Figure 3 were structured quadratic grid. The grid was also generated inside of the airfoil in order to perform conjugate heat transfer.

Table 1: Computational Mesh for NACA 0012 airfoil

Domain	**Nodes Around Airfoil**	**Total Number of Elements**
Level-1	120	322756
Level-2	240	600408
Level-3	480	925188

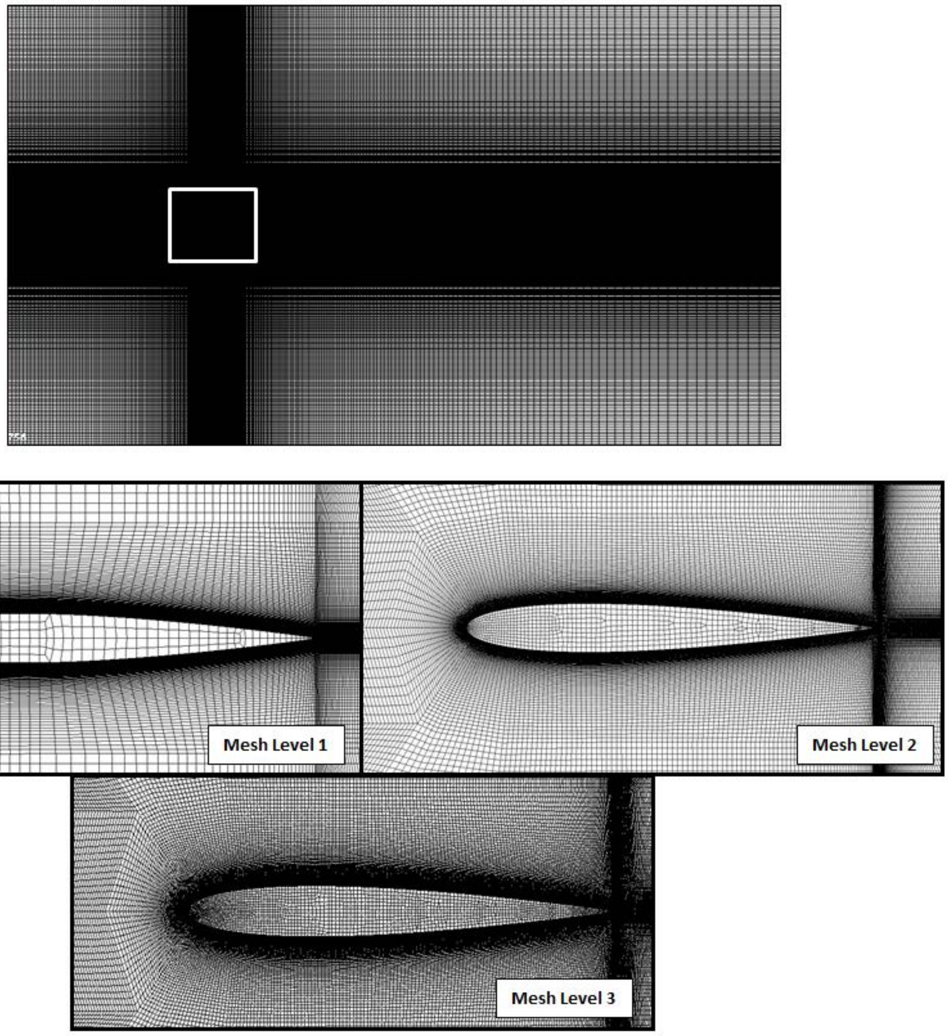

Figure 3: Computational Domain

Drag coefficient is defined as:

$$C_d = \frac{F}{\frac{1}{2}\rho U_\infty^2 c}$$

where F is drag per unit span, ρ is density, U_∞ is free stream velocity and c is chord length of airfoil. The drag coefficients obtained using different meshes are given in Figure 4. Drag coefficients are categorized into two main parts as pressure drag and viscous drag. Total drag is obtained basically by adding two drag coefficients:

$$C_d = C_{d,p} + C_{d,v}$$

where C_d is total drag coefficient, $C_{d,p}$ is pressure drag coefficient, $C_{d,v}$ is viscous drag coefficient. According to the Figure 4, the CFD results were matching with the test data of Sandia National Laboratory for drag coefficient of 1.7 Mach with angle of attack 0° that is 0.0065. It is observed that the results for Mesh Level 2 and Mesh Level 3 are very close to each other. The rest of study is performed with Mesh Level 3.

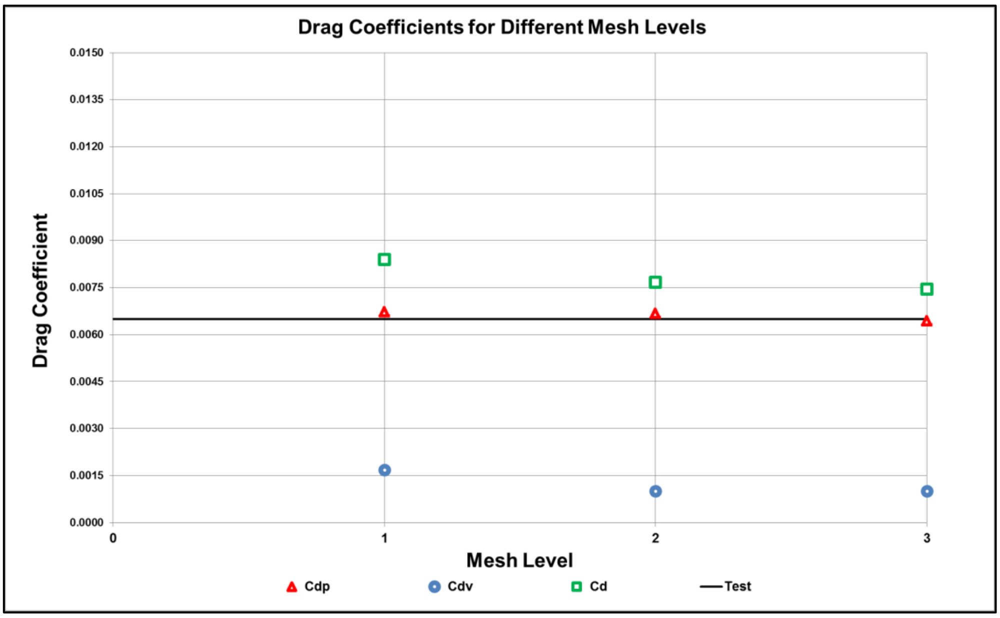

Figure 4: Drag Coefficients

2.3 Results

The aim of this work is to obtain the deformation rates of fins exposed to the high temperatures. The deformation rates on the fin were obtained a set of CFD and thermomechanical finite element analyses.
In the first step, heat transfer parameters and pressure distribution over the fin profile were determined from the CFD analysis. Then, these parameters were applied to finite element model as a boundary condition in order to obtain stress distribution on the fin body. It was investigated how fin was deformed by stress due to thermal and structural loadings. The procedure of analyses is demonstrated as a flowchart in Figure 5.

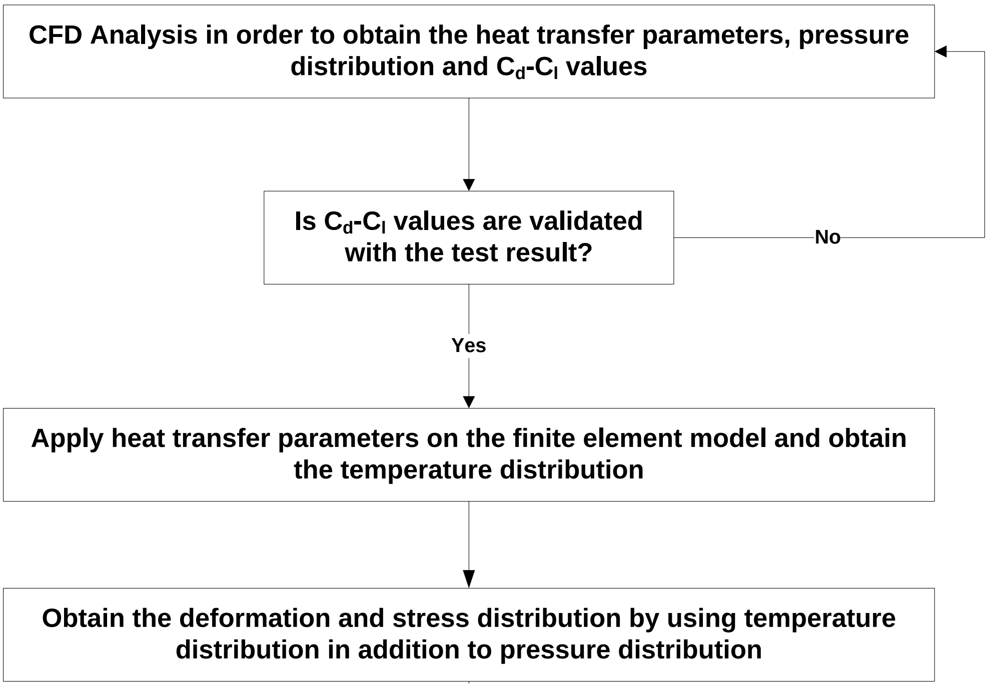

Figure 5: The Procedure of Analyses

2.3.1 Computational Fluid Dynamic Simulations

Simulations were done for three different Mach numbers in order to investigate the effect of flow conditions on the deformation on the airfoil. Static Pressure distribution along the airfoil is given in Figure 6. Heat transfer parameters (heat transfer coefficient and reference temperature) along the airfoil are given in Figure 7. These parameters were used as a boundary condition in finite element models.

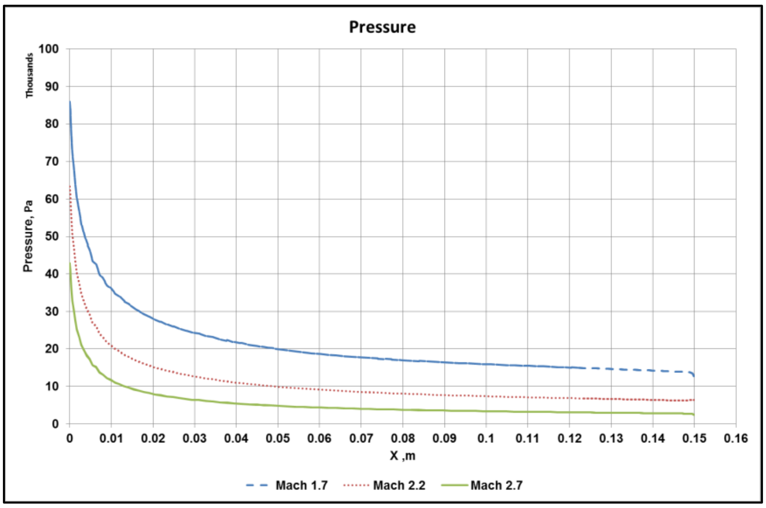

Figure 6: Static Pressure Distribution along the Airfoil

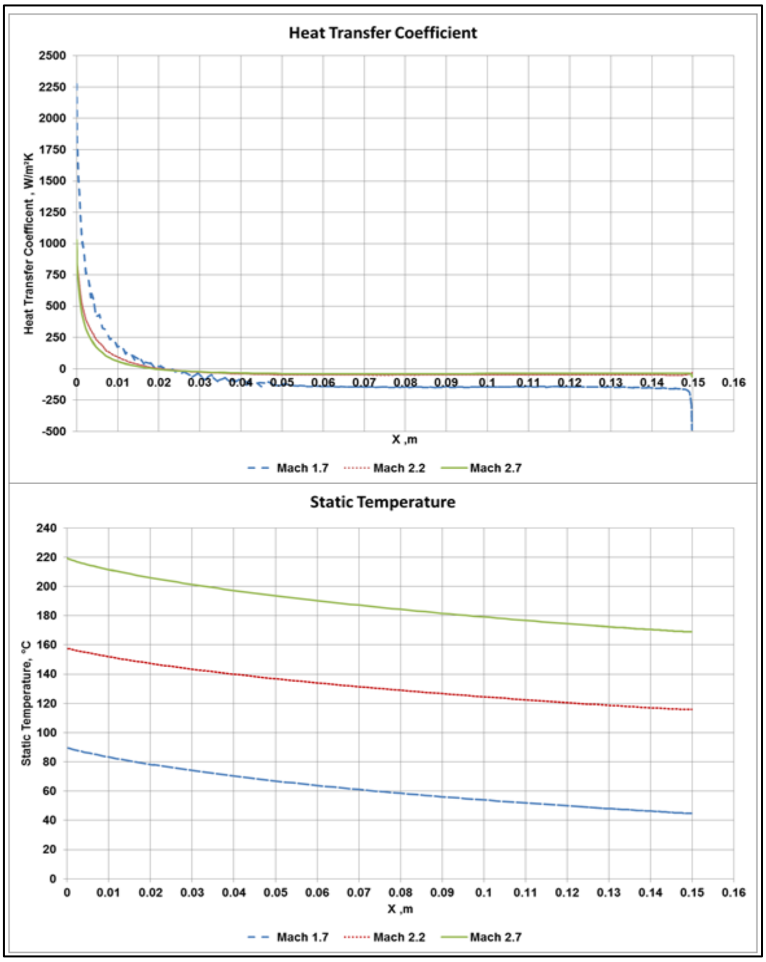

Figure 7: Heat Transfer Parameters along the Airfoil

2.3.2 Finite Element Simulations

In the finite element part of the simulations, a thermomechanic three dimensional finite element model of NACA 0012 fin body was generated and CFD analysis results of two-dimensional NACA 0012 airfoil were used as boundary condition. CFD analysis results were converted to a three dimensional form by using a basic Matlab script and then applied to the finite element model given in Figure 8.

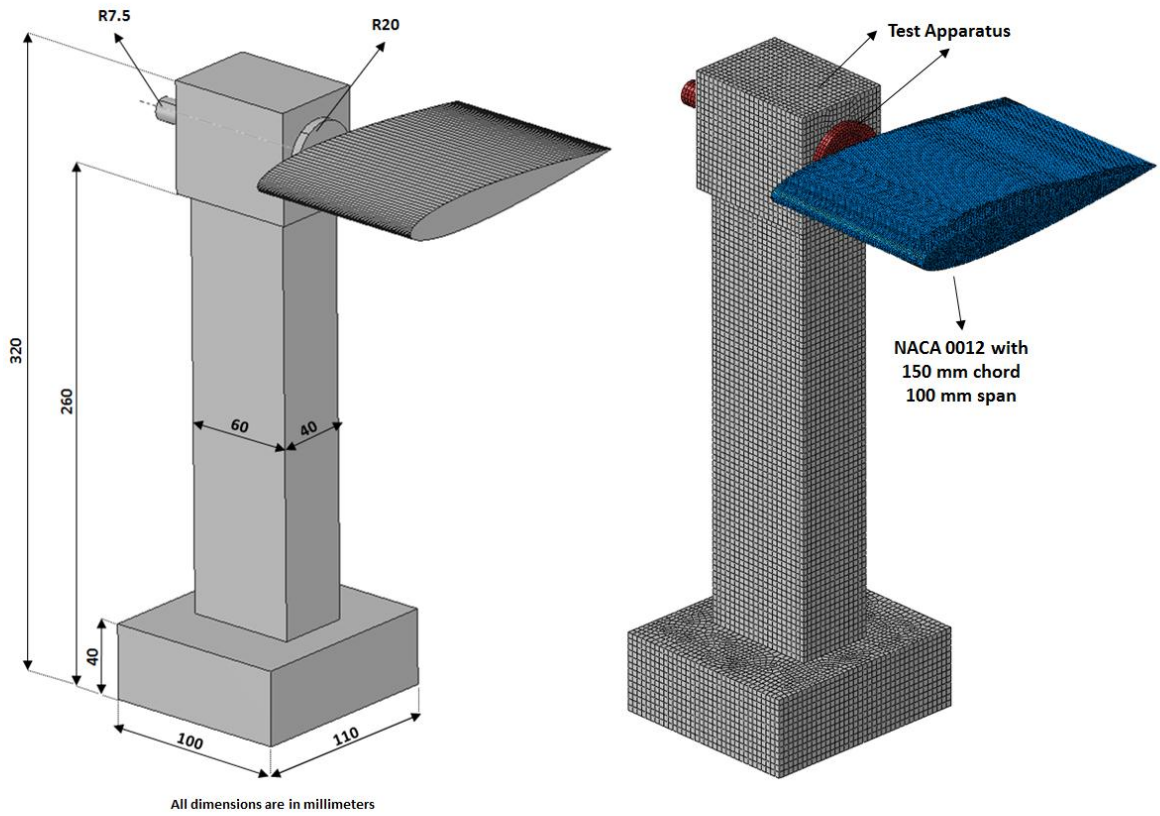

Figure 8: Finite Element Model of NACA 0012

Material properties of the fin and test apparatus used in the model are listed in Table 2. Surfaces where boundary conditions were applied are demonstrated in Figure 9. All of the contact surfaces of the model were modeled as a bounded contact.

Table 2: Material Properties for Finite Element Model

	Property	NACA 0012	Test Apparatus
Mechanical	**Density (kg/m^3)**	2770	7850
	Young Modulus (Pa)	72×10^9	200×10^9
	Poisson Ratio (-)	0.33	0.32
	Expansion (1/°C)	2.3×10^{-5}	1.17×10^{-5}
Thermal	**Conductivity (W/m.K)**	120	40
	Specific Heat (J/kg.°C)	910	400

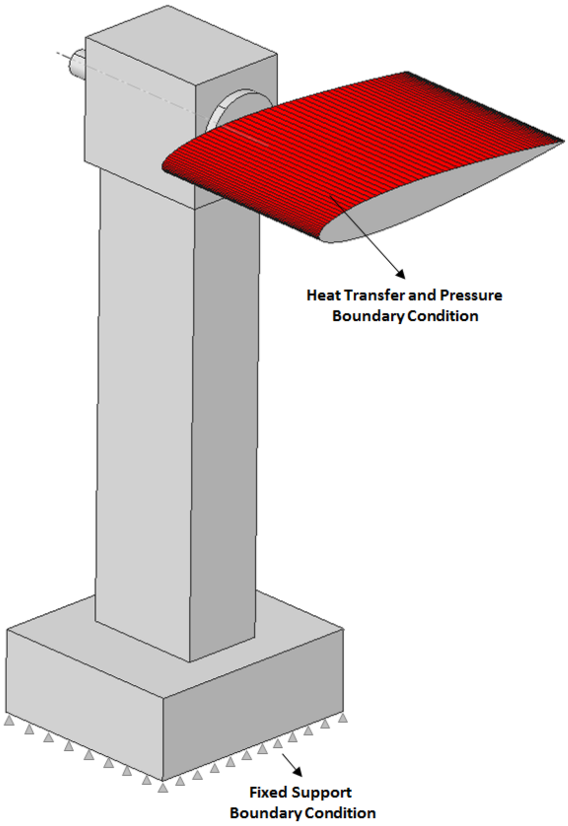

Figure 9: Boundary Conditions of the FE Model

Temperature distribution on the FE model solved for different Mach number conditions are given in Figure 10 and stress distribution is given in Figure 11. According to the Figure 11, it is clearly seen that maximum stress on the fin body occurs in the case of Mach Number 2.7.

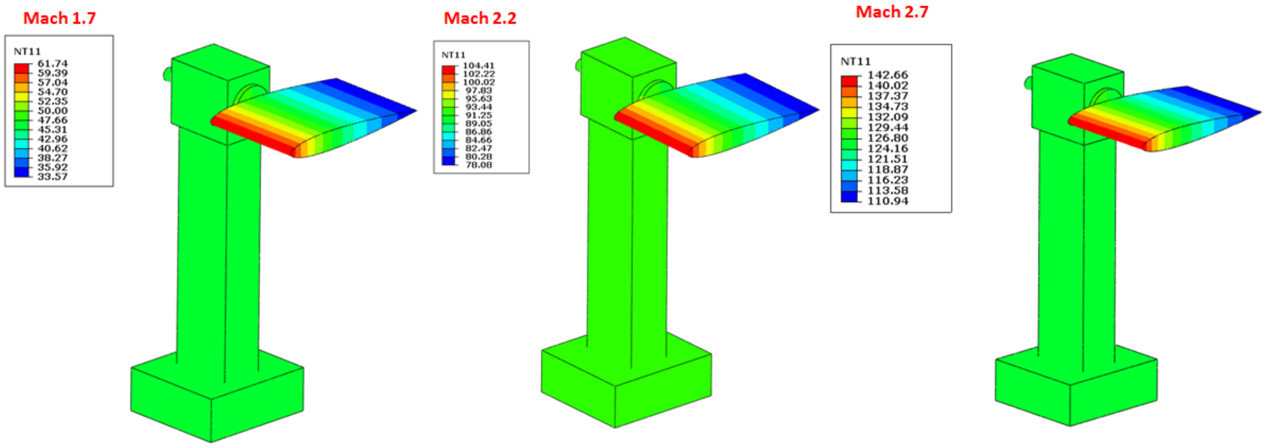

Figure 10: Temperature Distribution (°C) on the FE Model for Different Mach Numbers

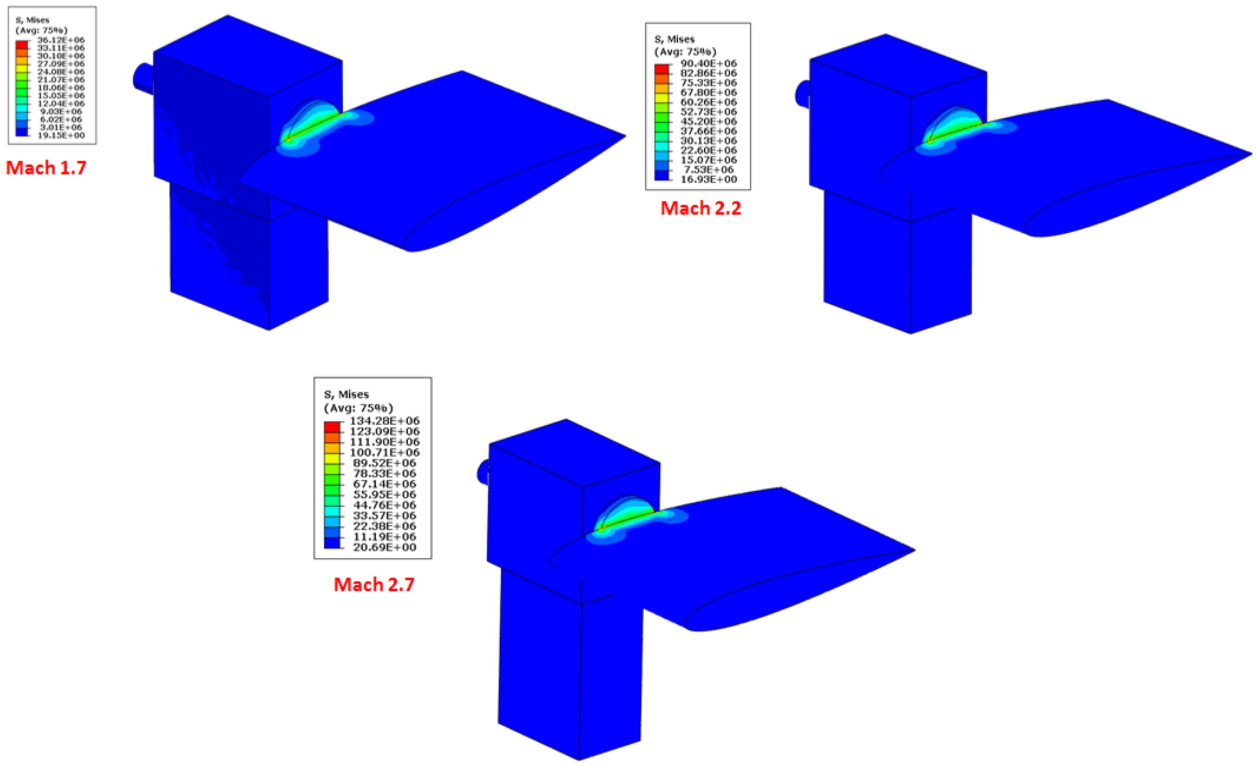

Figure 11: Stress Distribution (Pa) on the FE Model for Different Mach Numbers

3 Conclusion and Future Work

In this work, a methodology was developed to obtain the deformation rates and stress distributions on the airfoil surface exposed to the high temperatures. Results of CFD part were compared the test data from literature.

According to the results for the drag coefficients given in Figure 4, there is a difference between simulations and test data. In this study, the altitude was assumed to be zero, so density used in the CFD analysis was calculated at sea level conditions. A difference in altitude between the test conditions and simulation done can cause the difference in C_d calculations. Another reason is that smoothness and material properties of the test model could not be the same as the model used in this work. These parameters can also cause the difference.

For the future work, comparison of analysis results with different test results in order to obtain more accurate solution will be done and the CFD analysis will be repeated by using the deformed fin model.

References

[1] R. E. Sheldahl and P. C. Klimas, Aerodynamic Characteristics of Seven. Symmetrical Airfoil Sections Through. 180-Degree Angle of Attack for Use in. Aerodynamic Analysis of Vertical Axis Wind Turbines, Sandia National Laboratory, 1981

[2] Wright B.R., Bruckman F., Radovcich N.A., Arrow Wings for Supersonic Cruise Aircraft, Journal of Aircraft Vol.15, 12, 1978

[3] Sani A.S., Roohi E., Kahrom M., Stefanov S., Investigation of Aerodynamic Characteristics of Rarefiwld Flow Around NACA 0012 airfoil using DMSC and NS Solvers, European Journal of MechanicsB/Fluids Vol.48, 2014

[4] Martinat G., Braza M., Hoarau Y., Harran G., Turbulence Modelling of the Flow Past a Pitching NACA 0012 airfoil at 105 and 106 Reynolds Number, Journal of Fluids and Structures, Vol.24, 2008.

[5] Yemenici O., Experimental Investigation of the Flow Field around NACA 0012 Airfoil, International Journal of Sciences, Vol.2, 2013.

[6] Johansen J., Prediction of Laminar/Turbulent Transition in Airfoil Flows, Risø National Laboratory, 1997

[7] Michel R., Etude de la Transition sur les Profiles d'Aile; Etablissement d'un Critére de Determination de Point de Transition et Calcul de la Trainee de Profile Incompressible, Tech. rep. ONERA, Report 1/578A, 1958

[8] Miller D.S., Schemensky R.T., Design Study Results of a Supersonic Cruise Fighter Wing, AIAA 17th Aerospace Sciences Meeting, A79-19512, 1979

[9] Nangia R.K., Palmer M.E., Doe R.H., A Study of Supersonic Aircraft with Thin Wings of Low Sweep, AIAA 40th Aerospace Sciences, 2002-0709, 200219512, 1979

[10] Sakata I.F., Davis G.W. Robinson J.C., Yates E.C., Design Study of Structural Concepts for an Arrow-Wing Supersonic-Cruise Aircraft, AIAA Aircraft Systems and technology Meeting, M75-15607, 1975

[11] Wintzer M., Sturdza P.,Kroo I., Conceptual Design of Conventional and Oblique Wing Configurations for Small Supersonic Aircraft, AIAA 44th Aerospace Sciences Meeting and Exhibit, 2006-930, 2006

[12] Hoffman J., Jansson J., Jansson N., Simulation 3D Unteady Incompressible Flow Past a NACA 0012 Wing Section, Computational Technology Laboratory Report,KTH-CTL-4023, 2016

[13] ANSYS Fluent Theory and User Guide, ANSYS Inc.

[14] Kurtulus, D.F., David, L., Farcy, A., Alemdaroglu, N., On the Unsteady Behavior of the Flow Around NACA 0012 Airfoil with Steady External Conditions at Re=1000, International Journal of Micro Air Vehicles, Vol.7 / No.3, 2015

[15] NACA Technical Memorandum 4741, Computer Program To Obtain Ordinates for NACA Airfoils, December 1996.